FIRST EXPERIENCES WITH CONTINENTAL SLOPE FOOT-LINE DETERMINATION FROM REAL BATHYMETRIC DATA

Petr Vaníček, David E. Wells, Tianhang Hou, and Ziqiang Ou
Department of Geodesy and Geomatics Engineering
University of New Brunswick
P.O. Box 4400
Fredericton, N.B., CANADA E3B 5A3

ABSTRACT

Earlier this year, we reported on a pilot study, designed to test the algorithm for maximum curvature surface determination developed at the University of New Brunswick (UNB), that was conducted on three relatively short stretches of the suspected foot-line. These stretches, selected from Canada's continental slope off its east coast, vary widely both in bottom morphology and in bathymetric data coverage. The morphology of the slope ranges from very gradual to very abrupt changes in gradient, including the Laurentian Fan, a multiple canyon-like structure. The data coverage also varies from single ship's tracks to very dense multi-beam data collected using the SEABEAM system. On these cases, we showed how data sampling and spacing affect the detection of the foot-line under different morphological regimes. In this paper, we discuss the results of our continued investigations.

INTRODUCTION

In our paper [Vaníček et al., 1994b], we reported on the initial steps we had taken towards a systematic investigation of the geometrical aspects of the continental slope foot-line determination. This being a report on the continuation of our investigation, we repeat the definitions and the findings here, before reporting the new findings. The patient reader, who is already familiar with the cited paper, will find some of the material repeated here.

The United Nations Conference on the Law of the Sea III (UNCLOS III) [United Nations, 1983, pp. 27-28] Article 76, Section 4(b) defines the foot of continental slope as "...the point of maximum change in the gradient at its base." In mathematics, the change in the gradient is called the curvature. The UNCLOS III document thus speaks of the foot of the continental slope as the point (at its base) at which the curvature is at the maximum. In our discussion here, we define additionally the foot-line as the line that connects all the foot-points. We thus understand the continental slope foot-line to consist of all the points, where the curvature of the slope, at its base, is at the maximum. We focus our attention exclusively on this purely geometrical aspect as described

above, ignoring the complications of geological and geophysical origin arising when the foot-line is covered with sediments of a certain thickness.

How can the foot-line be traced? To the best of our knowledge, all the attempts up to now used the bathymetric surface (the graphical image of the sea bottom constructed from bathymetric data) directly. In some cases, the human eye can trace the points of maximum curvature rather well, in other cases, it is next to impossible to do this. In all the cases, such tracing is subjective and no two people will come up with the same result. If an objective determination of the foot-line is desired, a different approach must be used.

We have investigated one such approach, based on realizing the legal definition of the foot in the UNCLOS III as closely as possible, whereby we construct the surface of maximum curvature (SMC for brevity) and trace the ridges (i.e., lines of maximum curvature!), if they exist, on this surface. The tracing of the ridges can be done automatically, i.e., objectively, and this is the reason why we became interested in this technique. We note that such automated tracing had not been implemented in our earlier software, and the plots showing our results obtained from real bathymetric data have had the ridges drawn by hand. In our subsequent investigations, where we have used simulated bathymetric data, an automatic detection of the ridges has already been implemented.

CONSTRUCTION OF THE SURFACE OF MAXIMUM CURVATURE

The SMC has to be constructed from available bathymetric soundings, such as those shown in Figures 1 and 2. The mathematical formulae for the maximum normal curvature (the two-dimensional equivalent of the uni-dimensional curvature used in the UNCLOS III definition is the normal curvature of the surface) use the first and second partial derivatives of the bathymetric surface. These are evaluated from bathymetric soundings. For the actual mathematical formulation the reader is referred to Vaníček et al. [1994a].

The maximum curvature values can be evaluated either at the locations of the available soundings, or on some selected, regular or irregular, grid of points. The former option is preferred because it best honours the collected data. The latter option implies the use of some approximation or interpolation and artifacts caused by the used approximation or interpolation technique may be expected to occur. Unfortunately, the preferred option may not give the optimal results either, if the bathymetric data density and configuration are not appropriate for the sea bottom morphology in the location. We shall address these problems in the next paragraph.

Before we do that, let us point out another aspect of the foot-line determination: What happens if the change in continental slope curvature is very gradual? This situation will cause a very gentle ridge on the SMC. In the extreme case, when the curvature is constant, the ridge will disappear altogether, the foot-line cannot be located

following the wording of Article 76, section 4(b), and an alternative such as the one suggested in United Nations [1993], has to be used.

The uncertainties in collected soundings can be propagated into the uncertainties of the SMC and, ultimately, into the uncertainties of the ridge tracing. Statistically derived standard deviations of maximum curvature values based on standard deviations of collected soundings are routinely determined by our software but not shown in our plots here; we shall not discuss this aspect of our work in this contribution.

PROBLEMS WITH ACTUAL SOUNDING DISTRIBUTIONS

When the location configuration of collected soundings is highly irregular (cf. Figure 1), the SMC computed at these locations may be affected by artifacts caused by the computational technique: the partial derivatives evaluated at the actual locations from surrounding soundings would not be representative of the bathymetric surface as such. An example of such artifacts is shown in Figure 3.

When the density of collected soundings is too high for the sea bottom morphology, small bottom features cause the values of maximum curvature to become too large. These large values then dominate the SMC, masking the gentler ridge associated with the continental slope foot-line — cf. Figure 4. Conversely, the collected soundings may also be too sparse for a meaningful determination of the foot-line. This can be easily understood and we do not offer any example of this case here.

Clearly, the answer to these problems is to match the data density with the sea bottom morphology and use as regular a data distribution as possible. When the available data coverage is too thin and/or too irregular, there exists no mathematical technique to remedy the situation — more data have to be collected. When a denser than necessary data coverage is available, this can be happily achieved. We shall discuss this in the next section.

DATA REGULARIZATION

The technique that has worked well with the three data sets we investigated is the areal data averaging. The idea of this technique is to divide the region of interest into small regular cells, evaluate the centroid of all the data locations in each cell, and associate a representative depth with the centroid. The representative depth is best chosen as a weighted average of all the soundings that fall within the cell, where the weight is selected to be inversely proportional to the distance between the sounding to be weighted and the centroid. We note that this process is not equivalent to equidistant data gridding. Rather, it results in a thinner, yet still irregular, coverage as seen in Figure 5 that shows the areal averaging of the actual data set from Figure 1 using cells of 0.4 by 0.4 degrees.

The only artifact created by this areal averaging is a smoothing of the bathymetric surface. If the size of the averaging cell is selected properly, then the areal averaging alleviates both problems described in the previous paragraph. Just what constitutes the proper size of a cell, depends on the sea bottom morphology. More numerical experimentation is needed before a definite prescription can be formulated. As an illustration, Figure 6 shows the SMC constructed from the regularized data set in Figure 5, while Figure 4 shows the SMC for the same data set but averaged on 0.1 by 0.1 degree cells.

One may now ask, of course, the obvious question: Having at least partially abandoned the principle of honouring the collected data, may other approximation, interpolation, or gridding schemes work just as well? The answer at this point must be yes; based on our limited experience, we have to leave this question open to further investigation. At this point, however, we want to look at how the goodness of the foot-line detection algorithm responds to bathymetric data quality variations.

AN EXPERIMENT WITH SYNTHETIC DATA

In this section, we describe an illustrative experiment which we have conducted using synthetic data. Figure 7 shows a "bathymetric" surface generated by an analytical formula (not given here) on a regular rectangular grid of 50 by 50 points, viewed from the northeast. As the surface was generated by an analytical formula, we could and did compute the foot-line analytically; the trace of the foot-line in the horizontal plane is shown in Figure 8. Also shown in Figure 8 is a trace of another line, plotted from points of maximum curvature determined from profiles running down the slope, parallel with the horizontal (west-east running) axis of the plot, i.e., from two-dimensional cross-sections of the surface as opposed to the three-dimensional SMC. We can see quite clearly that the two results are different. This should be borne in mind in practical applications.

Next, we perturbed the regular grid to simulate a bathymetric surface one would obtain using real bathymetric data through areal averaging (the plot is not shown here due to space limitations). The SMC constructed from this surface is plotted in Figure 9, viewed again from the northeast. The ridges of the maximum curvature are clearly visible — those corresponding to the foot-line as well as those corresponding to the gullies that run down the slope from west to east. These ridges can be traced quite easily in the horizontal plane, and Figure 10 shows the points (by circles) identified by a simple ridge tracing algorithm as lying on these ridges. The correct theoretical location of the foot-line is shown by the solid curve. Clearly, the recovery of the foot-line through the SMC is quite successful.

Further, to simulate an uneven sea bottom as well as errors in bathymetric observations, we have perturbed the "bathymetric" data by a random Gaussian noise with a zero mean and a standard deviation equal to 0.01 division on the vertical scale. The plot of this perturbed bathymetric surface, on the perturbed grid, is shown in Figure 11. Even though the introduced perturbations are quite small, the SMC corresponding to the perturbed surface, Figure 12, is rather distorted, in comparison with the SMC of

the unperturbed surface, cf. Figure 9. Indeed, the traces of the ridges are almost obliterated; this fact is seen perhaps even better in Figure 13, which shows the traces (dots) as determined by the ridge identification algorithm. This is a convincing illustration of the known principle in experimental sciences: taking a derivative of noisy observed data magnifies the noise. The phenomenon is even more pronounced when second derivative is used which, of course, is our case.

We thus have tried to smooth the SMC, using the two-dimensional moving average filter, involving the 8 immediately neighbouring points. As expected, this technique helps to make the ridges stand out more clearly. After applying this technique twice, we obtained a SMC shown in Figure 14, which represents a marked improvement over the original SMC in Figure 12. Applying the ridge detection algorithm to this SMC, we get the reasonable results displayed (by circles) in Figure 13.

CONCLUSIONS

It is naturally difficult to draw any definite conclusions from the very limited number of experiments described in this contribution. We can, however, offer a few observations which may prove useful in further work in the context of continental slope foot-line determination.

First, it may not always be the best strategy for the purpose of foot-line determination, to collect indiscriminately as much bathymetric data as possible. If the sea bottom is rough, or if the data noise is significant, the use of high density bathymetric data will result in spurious peaks in the SMC which will mask the location of the foot-line ridge. The inverse problem of having too thin and/or irregular a data coverage does not need any elaboration.

The natural tendency among experimental scientists to avoid artificial modelling represented by employing approximation, interpolation, or filtering — to "honour the data" — may not pay off here. Some modelling may be inevitable simply because the "noise" in the data, due to the roughness of the sea bottom and/or to errors in soundings, may act to destroy the curvature information in the data. At the very least, smoothing of either the bathymetric surface or the SMC may be necessary. Just what kind of modelling would introduce the least amount of subjectivity into the process remains to be seen. This leaves the door wide open to further investigations by means of both artificial and real bathymetric data.

Generally, the use of a SMC, as the tool that most closely reflects the wording of Article 76 of the UNCLOS III, should be adopted. We have shown that the location of the foot-line changes significantly when two-dimensional profiles of the slope are used instead of the maximum normal curvature determined from three-dimensional data.

We have not discussed the question of the foot-line uncertainty here, even though we had already developed appropriate algorithms to evaluate the uncertainty. This question too needs some elaboration and further investigation.

REFERENCES

United Nations, 1983. *UNCLOS*. New York.

United Nations, 1993. *The Law of the Sea: Definition of the Continental Shelf*. New York.

Vaníček, P., D.E. Wells, and Tianhang Hou, 1994a. Determination of the foot of the continental slope. Contract Report for Geological Survey of Canada, Atlantic Geoscience Centre, Dartmouth, N.S.

Vaníček, P., D.E. Wells, and Tianhang Hou, 199 b. Continental slope foot-line determination: Geometrical aspects. *Proceedings of the LOS Article 76 Workshop*, Ed. W. Wells, Fredericton, N.B., 14-15 April, Department of Geodesy and Geomatics Engineering, University of New Brunswick, pp. 57-67.

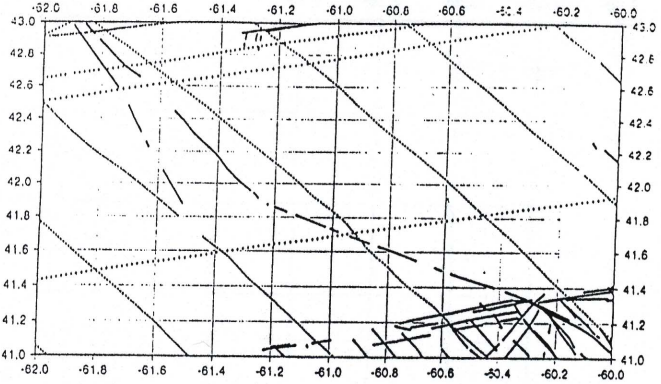

Figure 1: Single ship-track bathymetric data points collected off Canada's east coast. Numbers along the axes show the geographical latitude and longitude.

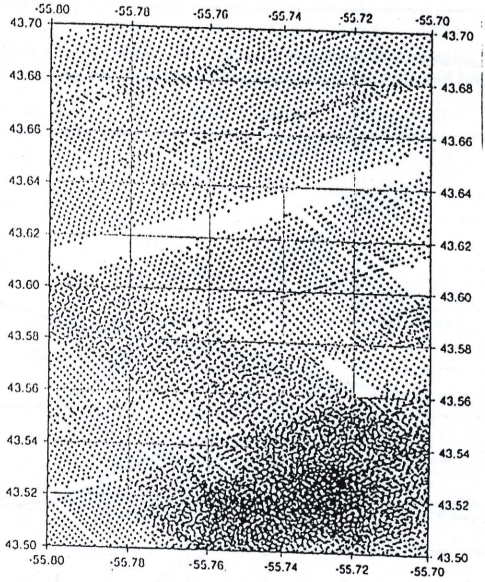

Figure 2: Multi-beam bathymetric data points collected off Canada's east coast with the SEABEAM system. Numbers along the axes show the geographical latitude and longitude.

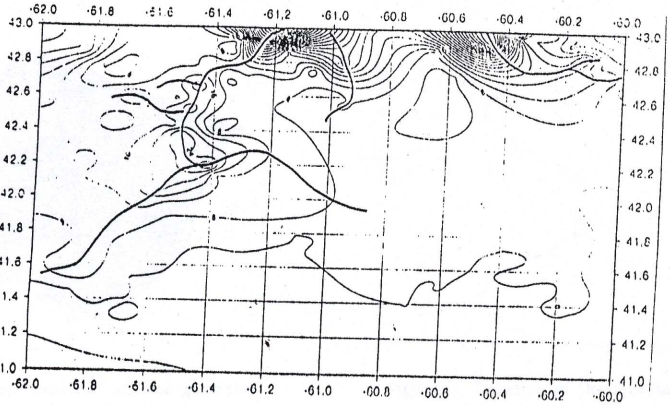

Figure 3: The Surface of Maximum (normal) Curvature (SMC) for the bathymetric data set displayed in Figure 1. Numbers along the axes show the geographical latitude and longitude. Note the artifacts along the northern edge of this plot.

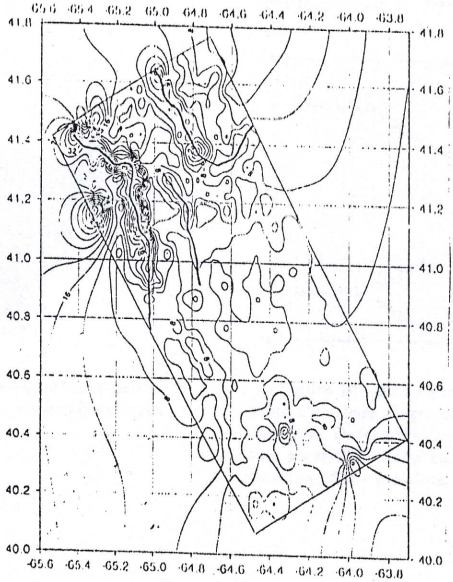

Figure 4: The SMC for another set of bathymetric data (not shown here) collected off Canada's east coast. Numbers along the axes show the geographical latitude and longitude.

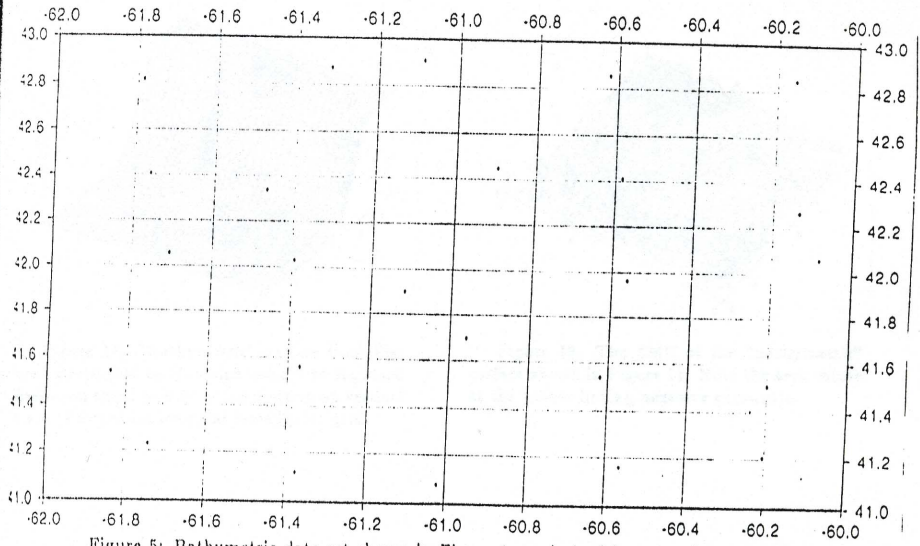

Figure 5: Bathymetric data set shown in Figure 1 regularized by averaging over 0.4 by 0.4 degree cells. Numbers along the axes show the geographical latitude and longitude.

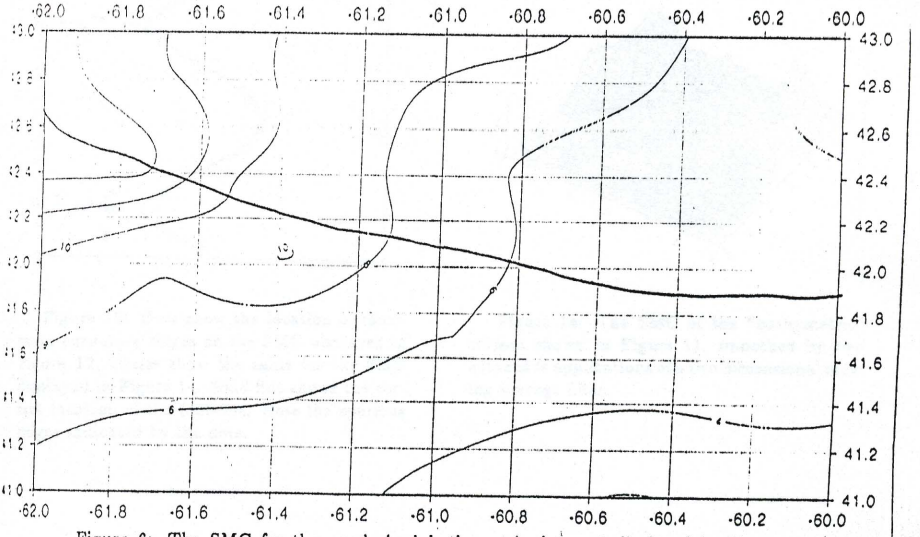

Figure 6: The SMC for the regularized bathymetric data set displayed in Figure 5. Numbers along the axes show the geographical latitude and longitude.

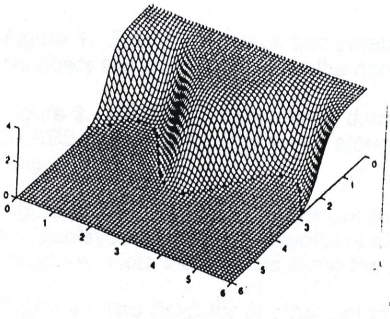

Figure 7: "Bathymetric" surface generated by an analytical expression plotted on a regular rectangular grid. Viewed from north-east. The location of the foot-line shown by asterisks.

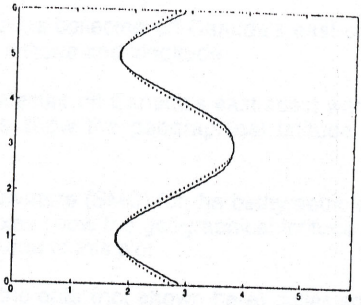

Figure 8: Location of the foot-line; correct, analytically determined location shown by solid line, location computed from east-west running two dimensional profiles shown by dots. Numberings along x-axis from west to east, along y-axis from south to north.

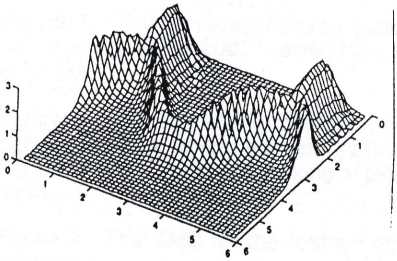

Figure 9: The SMC for the "bathymetric" surface displayed in Figure 7. Viewed from north-east.

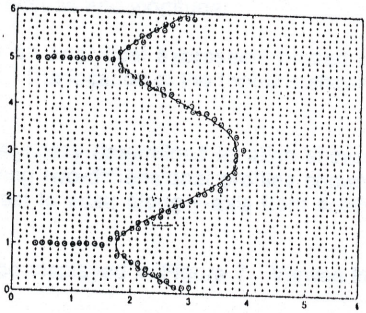

Figure 10: Circle show the location of maximum curvature ridges on the SMC displayed in Figure 9. Determination by a simple ridge location algorithm. Solid curve indicates the correct location of the foot-line.

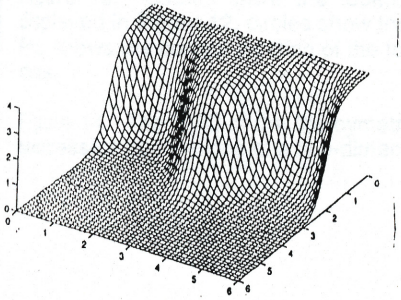

Figure 11: "Bathymetric" surface from Figure 7 perturbed by Gaussian noise with standard deviation equal to 0.01 of the division on vertical scale. Plotted on irregular rectangular grid.

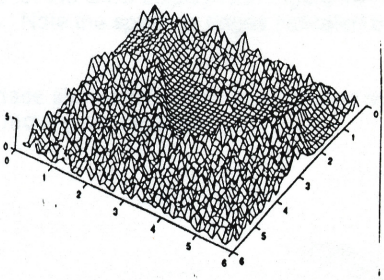

Figure 12: The SMC of the "bathymetric" surface shown in Figure 11. Note the zero values at the points having negative curvature.

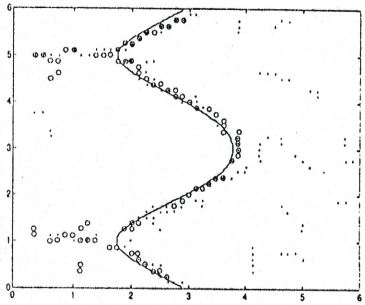

Figure 13: Dots show the location of maximum curvature ridges on the SMC displayed in Figure 12, circles show the same for the SMC displayed in Figure 14. Solid line shows the correct location of the foot-line. Note the spurious ridges indicated by the dots.

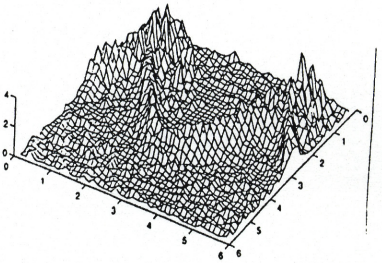

Figure 14: The SMC of the "bathymetric" surface shown in Figure 11, smoothed by two successive applications of a two dimensional moving average filter.

Figure captions

Figure 1. Single ship track bathymetric data points collected off Canada's east coast. Numbers along the axes show the geographical latitude and longitude.

Figure 2. Multibeam bathymetric data points collected off Canada's east coast with the SEABEAM system. Numbers along the axes show the geographical latitude and longitude.

Figure 3. The Surface of Maximum (normal) Curvature (SMC) for the bathymetric data set displayed in Figure 1. Numbers along the axes show the geographical latitude and longitude. Note the artifacts along the northern edge of this plot.

Figure 4. The SMC for another set of bathymetric data (not shown here) collected off Canada's east coast. Numbers along the axes show the geographical latitude and longitude.

Figure 5. Bathymetric data set shown in Figure 1 regularized by averaging over 0.4 by 0.4 degree cells. Numbers along the axes show the geographical latitude and longitude.

Figure 6. The SMC for the regularized bathymetric data set displayed in Figure 5. Numbers along the axes show the geographical latitude and longitude.

Figure 7. "Bathymetric" surface generated by an analytical expression plotted on a regular rectangular grid. Viewed from northeast. The location of the foot-line shown by asterisks.

Figure 8. Location of the foot-line; correct, analytically determined location shown by circles, location computed from east-west running two-dimensional profiles shown by the solid line. Numbering along x-axis from west to east; along y-axis from south to north.

Figure 9. The SMC for the "bathymetric" surface displayed in Figure 7. Viewed from northeast.

Figure 10. Circles show the location of maximum curvature ridges on the SMC displayed in Figure 9. Determination by a simple ridge location algorithm. Solid curve indicates the correct location of the foot-line.

Figure 11. "Bathymetric" surface from Figure 7 perturbed by Gaussian noise with standard deviation equal to 0.01 of the division on vertical scale. Plotted on irregular rectangular grid.

Figure 12. The SMC of the "bathymetric" surface shown in Figure 11. Note the zero values at the points having negative curvature.

Figure 13. Circles show the location of maximum curvature ridges on the SMC displayed in Figure 12, circles show the same for the SMC displayed in Figure 14. Solid line shows the correct location of the foot-line. Note the spurious ridges indicated by the dots.

Figure 14. The SMC of the "bathymetric" surface shown in Figure 11, smoothed by two successive applications of a two-dimensional moving average filter.